



**HAL**  
open science

# Hyaluronan: the absence of amide-carboxylate hydrogen bonds and the chain conformation in aqueous solution are incompatible with stable secondary and tertiary structure models

Charles D Blundell, Paul L Deangelis, Andrew Almond

► **To cite this version:**

Charles D Blundell, Paul L Deangelis, Andrew Almond. Hyaluronan: the absence of amide-carboxylate hydrogen bonds and the chain conformation in aqueous solution are incompatible with stable secondary and tertiary structure models. *Biochemical Journal*, 2006, 396 (3), pp.487-498. 10.1042/BJ20060085 . hal-00478515

**HAL Id: hal-00478515**

**<https://hal.science/hal-00478515>**

Submitted on 30 Apr 2010

**HAL** is a multi-disciplinary open access archive for the deposit and dissemination of scientific research documents, whether they are published or not. The documents may come from teaching and research institutions in France or abroad, or from public or private research centers.

L'archive ouverte pluridisciplinaire **HAL**, est destinée au dépôt et à la diffusion de documents scientifiques de niveau recherche, publiés ou non, émanant des établissements d'enseignement et de recherche français ou étrangers, des laboratoires publics ou privés.

**Hyaluronan: the absence of amide-carboxylate hydrogen bonds and the chain conformation in aqueous solution are incompatible with stable secondary and tertiary structure models**

Charles D. Blundell<sup>\*</sup>, Paul L. DeAngelis<sup>†</sup> and Andrew Almond<sup>\*‡</sup>

<sup>\*</sup>Faculty of Life Sciences, Manchester Interdisciplinary Biocentre, University of Manchester, 131 Princess Street, Manchester, M1 7ND, UK; <sup>†</sup>Department of Biochemistry and Molecular Biology, University of Oklahoma Health Sciences Center, Oklahoma 63104, USA.

<sup>‡</sup>Corresponding author. Tel.: +44 161 30 64 199; fax: +44 161 236 0409; email: andrew.almond@manchester.ac.uk

**Short title:** NMR analysis of hyaluronan secondary and tertiary structure models

## Synopsis

Contradictory descriptions for the aqueous solution conformation of the glycosaminoglycan hyaluronan (HA) exist in the literature. According to hydrodynamic and simulation data, HA molecules are stiffened by a rapidly-interchanging network of transient hydrogen bonds at the local level and do not significantly associate at the global level. In marked contrast, models derived from NMR data suggest that the secondary structure involves persistent hydrogen bonds and that strong associations between chains can occur to form vast stable tertiary structures. These models require an extended two-fold helical conformation of the HA chain and specific hydrogen bonds between amide and carboxylate groups. To test these descriptions, we have used  $^{15}\text{N}$ -labelled oligosaccharides and high-field NMR to measure pertinent properties of the acetamido group. The amide proton chemical shift perturbation and carboxylate group  $\text{p}K_{\text{a}}$  value are inconsistent with a highly populated hydrogen bond between the amide and carboxylate groups. Amide proton temperature coefficients and chemical exchange rates confirm this conclusion. Comparison of oligomer properties with polymeric HA indicates there is no discernible difference in amide proton environment between the centre of octasaccharides and the polymer, inconsistent with the formation of tertiary structures. A  $[^1\text{H}-^1\text{H}-^{15}\text{N}]$  NOESY-HSQC spectrum recorded on a HA octasaccharide revealed that amide groups in the centre are in a *trans* orientation and that the average solution conformation is not an extended two-fold helix. Therefore, the two key aspects of the secondary and tertiary structure models are unlikely to be correct. Rather, these new NMR data agree with descriptions from hydrodynamic and simulations data.

## Introduction

The glycosaminoglycan hyaluronan (HA) comprises repeated disaccharide subunits of *N*-acetyl-D-glucosamine (GlcNAc) and D-glucuronic acid (GlcA) (Figure 1A). It is synthesised as molecules of mass range  $10^5$  to  $10^7$  Da, although it is found as oligosaccharides in some physiological and pathological conditions [1, 2]. Diverse biological roles have been attributed to HA, mostly in extracellular and pericellular matrices. It is crucial to the organization of proteoglycan aggregates [3], formation of the matrix surrounding oocytes [4] and has many receptor-mediated roles in cell migration, adhesion, signalling and division [5]. However, a detailed molecular description of its solution three-dimensional structure, which is crucial to a full understanding of these biological processes, has been both elusive and controversial.

Viscometric and diffusion coefficient analyses have concluded that polymeric HA acts as a stiffened, worm-like coil, with a persistence length of 4 – 10 nm [6] and does not form significant intermolecular interactions in physiological solution [7]. The local stiffening responsible for generating the persistence length is believed to be a network of inter-residue hydrogen bonds (often referred to as the ‘secondary structure’ [8]) and was originally inferred from a reduced rate of periodate oxidation compared to other glycosaminoglycans and a reversible loss of viscosity at pH values above the  $pK_a$  of the hydroxyl groups [9]. Data from NMR, however, indicate that there are no stable long-lived inter-residue hydrogen bonds in oligomers and that co-operative intramolecular hydrogen bonds play a minor role in determining the local chain conformation [10-13]. Reconciling these apparently opposing views, molecular dynamics simulations tend to suggest that both intramolecular hydrogen bonds and bridging water molecules between residues are indeed prevalent and affect the conformation of HA, but are short-lived, frequently interchanging on the picosecond timescale [7, 14, 15]. The most controversial inter-residue hydrogen bond is that proposed to exist between GlcNAc amide hydrogen atoms and adjacent GlcA carboxylate groups in the same HA chain (see Figure 1B) [10-12, 16]. While these intramolecular hydrogen bonds are present in HA oligomers in dimethyl sulphoxide (DMSO) solution [17], in aqueous solution they appear to be disrupted by H<sub>2</sub>O molecules that hydrogen bond to both groups, forming a water-bridge (see Figure 1C) [18].

As a result of these controversies, there are currently three different descriptions in the literature for the secondary structure of HA in aqueous solution. The original model is identical to that of HA in DMSO solution [17], having a highly populated intramolecular amide-carboxylate hydrogen bond (as in Figure 1B) and an extended two-fold helical conformation (glycosidic angles  $\beta(1\rightarrow3)$ :  $\varphi_H = 34^\circ$ ,  $\psi_H = -13^\circ$ ;  $\beta(1\rightarrow4)$ :  $\varphi_H = 13^\circ$ ,  $\psi_H = -29^\circ$ ); this will be referred to as the TF-INTRA model (for two-fold and intramolecular). A subsequent, revised model also has an extended two-fold helical conformation, but replaces the intramolecular hydrogen bond with a tightly and persistently bound water molecule bridging the amide and carboxylate groups (as in Figure 1C) [18]; this will be referred to as the TF-WB model (for two-fold and water-bridged). In contrast, the secondary structure according to molecular dynamics simulations (the DYN model, for dynamic) [7, 14, 15] is described as rapidly fluctuating between a range of helical conformations with amide and carboxylate groups being in rapid interchange between infrequent, weak intramolecular amide-carboxylate hydrogen bonds and ubiquitous but weakly-bound water-bridged states. In

order to test these models, experimental information on 1) the aqueous helical conformation of HA and 2) the strength and persistence of intramolecular amide-carboxylate hydrogen bonds and water-bridging arrangements is required.

In this regard, Nuclear Overhauser effect (NOE) intensities from HA octasaccharides were measured in an initial attempt to determine the average solution helical conformation of HA, concluding that the  $\beta(1\rightarrow3)$  glycosidic linkage angles were  $\varphi_H = 46^\circ$ ,  $\psi_H = 24^\circ$  and two different sets of values were valid solutions to the data at the  $\beta(1\rightarrow4)$  linkage ( $\varphi_H = 24^\circ$ ,  $\psi_H = -53^\circ$  and  $\varphi_H = 48^\circ$ ,  $\psi_H = 8^\circ$ ) [19]. Deconvolution of the severely overlapped NOEs into distances is a significant challenge to the accuracy of this result, however, not least because end-effects and local chain dynamics affect the average distances between atoms. This result suggested that HA does not adopt an extended, two-fold helical conformation in aqueous solution and therefore cast doubt on this aspect of the TF-INTRA and TF-WB models. There are currently no experimental data available on the persistence of intramolecular hydrogen bonds and water-bridging arrangements in aqueous solution, preventing evaluation of these aspects of the secondary structure models.

A critical biological question is whether the HA polymer has a solution conformation similar to that of the oligomers. This is not only important for understanding the viscoelastic properties of the free polymer, but has implications for the capture and binding of proteins in the formation of extracellular matrix structures [20]. Suggestion that the polymer does have different conformational properties is supported by the observation that the  $^{13}\text{C}$  carbonyl resonance of the amide group experiences a considerable selective broadening in the polymer [21-23]. In order to explain these line-width data, polymeric HA in solution has been investigated by chemically modifying the *N*-acetyl sidechain groups; concomitant changes to the linewidth and chemical shift of this single resonance have been used to infer a tertiary structure [21]. This structure is proposed to form spontaneously in physiological conditions, and involves the coalescence of hyaluronan chains into vast, stable networks, in sharp contrast to the hydrodynamic data that have indicated no intermolecular interactions occur in physiological solution (*vide supra*).

A molecular model for the proposed stable tertiary structures has been put forward that involves HA chains stacking on top of each other in an antiparallel arrangement under co-

operative hydrogen-bonding and hydrophobic stacking interactions (see Figure 1D) [21-25]. In particular, the HA chains are required to adopt the extended two-fold helical conformation (from the TF-INTRA/TF-WB secondary structure models) to allow the tessellation of stacked hydrophobic patches. The tertiary structures are also proposed to be stabilised by intermolecular hydrogen bonds between the amide and carboxylate groups on adjacent stacked chains; this model will therefore be referred to as the TF-INTER-S tertiary model (for two-fold, intermolecular, stacking). If this description is correct, the NMR data it is based on indicate that a very high proportion of the amide groups are involved in such intermolecular interactions [21].

In order to perform new experiments to resolve these controversies, we have prepared variably-sized and  $^{15}\text{N}$ -isotopically-labelled oligomers that allow the measurement of properties at specific positions within HA molecules [5, 26]. Using these preparations, we investigate the proposed intramolecular, water-bridged and intermolecular hydrogen bond arrangements between the amide and carboxylate groups in the secondary and tertiary structure models and conclude that there is no evidence for any of these hydrogen bond arrangements being more than sparsely populated in solution. In addition, it is demonstrated that the conformation in (the centre of) HA octasaccharides and the polymer are very similar and do not adopt an extended two-fold helical conformation in solution. It is therefore concluded that the two properties foundational to the TF-INTRA/TF-WB secondary and TF-INTER-S tertiary structure models are inconsistent with the experimental data. However, these new data are compatible with the DYN model. It is also concluded that it is reasonable to transfer properties measured on octasaccharides into descriptions of the polymer, allowing for the development of a new atomistic account of the solution properties of high molecular-mass HA. Such an account will provide important new insights into the biology emergent from the polymer's solution behaviour and its interactions with proteins.

## Experimental

### *Sources and preparation of saccharides*

Medical grade HA (Hylumed Medical,  $M_r$  0.5 - 1.5  $\times 10^6$ ; HA<sub>2500-8000</sub>) was obtained from Genzyme (Boston, USA) and  $^{15}\text{N}$ -labelled high  $M_r$  HA was produced by *E. coli* transfected with recombinant HA synthase [5]. Even-numbered unlabelled and  $^{15}\text{N}$ -labelled HA oligosaccharides with GlcNAc at the reducing terminus (i.e., HA<sub>4</sub>, HA<sub>6</sub>, HA<sub>8</sub>, HA<sub>10</sub>, HA<sub>40</sub>) were prepared from these high  $M_r$  HA sources as described previously [5, 27].  $\Delta$ 4,5-

unsaturated tetrasaccharides ( $\Delta$ -HA<sub>4</sub>) were prepared in the same manner, but with the use of *Streptomyces hyaluronolyticus* hyaluronate lyase (Sigma-Aldrich, 300 units, 100 mg HA<sub>2500-8000</sub>, 4 days). The trisaccharide GlcNAc-GlcA-GlcNAc~OH (i.e., HA<sub>3</sub><sup>NN</sup>) was prepared by digestion of purified HA<sub>4</sub> with bovine liver  $\beta$ -glucuronidase (Sigma-Aldrich). The <sup>15</sup>N-labelled pentasaccharide with GlcA at both termini (i.e., <sup>15</sup>N-HA<sub>5</sub><sup>AA</sup>) was purified as a trace product from testicular hyaluronidase digests of the <sup>15</sup>N polymer [28]. Matrix-assisted laser desorption/ionization time-of-flight (MALDI-ToF) analysis was used to confirm the masses of oligosaccharide products [5].

#### *General NMR methodologies*

NMR samples contained 10 % (v/v) D<sub>2</sub>O, 0.02 % (w/v) NaN<sub>3</sub>. Spectra were acquired at pH 6.0 and 25 °C (unless otherwise stated) with a proton resonant frequency of 750 MHz and processed as described previously [5].

#### *Determination of carboxylate groups pK<sub>a</sub> values*

NMR spectra were recorded on oligosaccharide samples over the pH range 6.0 to 1.4, in 0.3-0.4 pH unit decrements. In the case of the unlabelled samples investigated (i.e., 3.9 mM HA<sub>3</sub><sup>NN</sup>, 3.0 mM HA<sub>4</sub>, 2.0 mM  $\Delta$ -HA<sub>4</sub>) 1D spectra were recorded with an acquisition time of 113.66 ms over 1024 complex points. For the <sup>15</sup>N-labelled oligomers (i.e., 0.5 mM <sup>15</sup>N-HA<sub>4</sub>, 0.5 mM <sup>15</sup>N-HA<sub>6</sub>), both 1D spectra and gradient-enhanced [<sup>1</sup>H-<sup>15</sup>N] HSQC datasets (acquisition time 1088.00 ms over 128 points in t<sub>1</sub>, <sup>15</sup>N; 113.66 ms over 1024 points in t<sub>2</sub>, <sup>1</sup>H; <sup>15</sup>N carrier frequency set to 122.5 ppm at pH 6.0) were acquired. The chemical shifts of resonances of interest were plotted as a function of pH after subtraction of the intrinsic change in chemical shift of GlcNAc with pH (~-3 ppb from pH 6.0 to 1.4). The resultant curves were fitted by nonlinear least-squares analysis to one-site models, giving a measurement of the apparent pK<sub>a</sub>(s) of the titrating group; two-site models were found to be unnecessary since the pK<sub>a</sub> of different carboxylate groups within the same HA oligomer were indistinguishable.

#### *Amide proton chemical shift*

1D spectra were recorded with the parameters described above on samples at pH 6.0 and 1.4 of the following concentrations: HA<sub>8</sub> 5 mM, HA<sub>40</sub> 0.8 mM (~13 mM internal disaccharides), HA<sub>2500-8000</sub> at 2 mg/ml, equivalent to 5 – 15 mM disaccharide units.

### *[<sup>1</sup>H-<sup>1</sup>H-<sup>15</sup>N] NOESY-HSQC spectrum of HA<sub>8</sub>*

A gradient-enhanced [<sup>1</sup>H-<sup>1</sup>H-<sup>15</sup>N] NOESY-HSQC spectrum (mixing time 400ms) was recorded on an 11.5 mM <sup>15</sup>N-HA<sub>8</sub> sample with the <sup>15</sup>N carrier frequency at 122.0 ppm and acquisition times of 17.06 ms (128 points) (t<sub>1</sub>, <sup>1</sup>H), 819.20 ms (32 points) (t<sub>2</sub>, <sup>15</sup>N) and 113.66 ms (1024 points) (t<sub>3</sub>, <sup>1</sup>H).

### *Measurement of [<sup>1</sup>H-<sup>15</sup>N] NOE enhancements*

The [<sup>1</sup>H-<sup>15</sup>N] NOE enhancement was measured for each amide resonance in <sup>15</sup>N-HA<sub>4</sub> (0.5 mM), <sup>15</sup>N-HA<sub>6</sub> (0.5 mM) and <sup>15</sup>N-HA<sub>8</sub> (1 mM) at pH 1.4, following the manner described previously [26].

### *Measurement of <sup>3</sup>J<sub>HH</sub> coupling constants*

The <sup>3</sup>J<sub>HH</sub> coupling constants between the H<sup>N</sup> and H<sup>2</sup> protons were determined by direct measurement from 1D and [<sup>1</sup>H-<sup>15</sup>N] HSQC spectra (sample concentrations 0.5 – 4.0 mM).

### *Determination of amide proton and nitrogen temperature coefficients*

Homonuclear 1D spectra were recorded on saccharide samples at 10 °C, 25 °C and 35 °C, referencing α and β H<sup>N</sup> resonances to internal DSS. [<sup>1</sup>H-<sup>15</sup>N] HSQC spectra were also recorded at these temperatures and were referenced using the α and β H<sup>N</sup> chemical shifts determined from the 1D spectra. Saccharide concentrations ranged from 0.5 – 12 mM, except in the cases of HA<sub>2500-8000</sub> samples (2 mg/ml) and GlcNAc [<sup>1</sup>H-<sup>15</sup>N] HSQC spectra at natural abundance (100 mM).

### *Fast-exchange experiments*

Fast-exchanging amide protons were monitored using an H<sub>2</sub>O-exchange-[<sup>1</sup>H-<sup>15</sup>N]-HSQC pulse sequence. This involved inverting the water resonance with selective shaped Wurst pulses, waiting for an exchange delay (10, 25, 50, 100, 200 ms) during which chemical exchange of water protons for amide protons occurred, and then performing a [<sup>1</sup>H-<sup>15</sup>N] HSQC. The phase cycle of the [<sup>1</sup>H-<sup>15</sup>N] HSQC step ensured that only magnetisation originating on water was detected in the final spectrum. The peak height of every resonance after each exchange delay was recorded and normalised to the βHN intensity at 200 ms (defined to be 100 %), including an appropriate scaling factor to account for the typical difference in intensity seen between the resonances in a [<sup>1</sup>H-<sup>15</sup>N] HSQC spectrum (e.g. for

HA<sub>6</sub>, the ratio of intensities of resonances  $\beta:\alpha:\gamma:\omega$  is 0.26:0.55:0.98:1.00). Relative exchange rates of the amide groups were then estimated from the initial gradient of the graph.

## Results

### *Carboxylate group pK<sub>a</sub> is inconsistent with amide-carboxylate hydrogen bonds*

NMR-monitored pH titrations can be used to identify hydrogen bonds between amide protons and carboxylate groups, which are often transiently populated. Previous studies on model peptides and proteins have shown that the proximity of the carboxylate group's negative charge induces polarization of the amide N-H bond with a consequent downfield shift of the amide proton resonance [29, 30]. As a minimum threshold, a downfield shift of ~250 parts per billion (ppb) is associated with a hydrogen bond that is populated ~20 % of the time, with higher values representing proportionally greater occupancies, to a very rough approximation [30]. The favourable charge stabilization arising from a hydrogen bond also results in the depression of the carboxylate pK<sub>a</sub> below its intrinsic value (typically  $\geq 0.3$  units). If a water molecule were tightly bound in a long-lived water-bridge between the amide and carboxylate groups, such an interaction would also be expected to decrease the pK<sub>a</sub> of the carboxylate group below its intrinsic value. In the case of HA oligosaccharides, the best reference compound for the carboxylate intrinsic value is not GlcA (pK<sub>a</sub> 3.20-3.25), but a 4-OH substituted GlcA to compensate for the inductive effect expected from substitution of a GlcNAc ring at this position in HA [31]. The intrinsic value for comparison will therefore be that of 2,3,4-trimethoxyl-GlcA, which has a pK<sub>a</sub> of 3.03 [31] (at 20 °C), and observed pK<sub>a</sub> values in HA oligosaccharides below 2.7-2.8 will constitute evidence that the carboxylate charge is stabilised by an additional intra- or intermolecular interaction (i.e., hydrogen bond).

Several pH titrations were performed on HA oligosaccharides of different structure, and it was observed that the amide resonances had pH-dependent variations in chemical shift (Figure 2A, B; all chemical shift data is reported in Supplementary Table 1). In the case of the trisaccharide HA<sub>3</sub><sup>NN</sup> (i.e., GlcNAc-GlcA-GlcNAc~OH, see Figure 3 for nomenclature), all three amide protons ( $\beta\text{H}^{\text{N}}$ ,  $\alpha\text{H}^{\text{N}}$ ,  $\omega\text{H}^{\text{N}}$ ) displayed perturbed chemical shifts as the carboxylate group changed its ionization state. Since this oligomer contains one ionizable group, all of these nuclei separately report its pK<sub>a</sub>, which was determined to be  $2.9 \pm 0.1$  by fitting the data to one-site models (Table 1); this value is clearly not significantly depressed relative to the intrinsic value of 2,3,4-trimethoxyl-GlcA. The  $\omega\text{H}^{\text{N}}$  resonance of HA<sub>3</sub><sup>NN</sup> does titrate

downfield upon protonation of the carboxylate group (see Figure 2A) but the magnitude of chemical shift change (140 ppb, Table 1) is considerably less than that required to be consistent with the loss of a significantly populated transient hydrogen bond. The  $\beta$  and  $\alpha$   $^1\text{H}^{\text{N}}$  resonances of  $\text{HA}_3^{\text{NN}}$  both display small upfield chemical shift perturbations (20 ppb) upon titration, indicating that they are not involved in a close interaction with the carboxylate group but simply report its change in ionization state. Therefore, these data are inconsistent with the existence of a significantly populated transient hydrogen bond between the amide and carboxylate groups (i.e., refuting the TF-INTRA model). Furthermore, these data do not support the hypothesis that a water molecule is tightly bound between them (i.e., refuting the TF-WB model). Titrations performed on the tetrasaccharide ( $\text{HA}_4$ ) and lyase-derived tetrasaccharide ( $\Delta\text{-HA}_4$ ) gave similar results and also revealed that the  $\text{p}K_{\text{a}}$  values of the two carboxylate groups in these molecules were indistinguishable (Table 1).

Chemical shift changes during pH titrations of  $^{15}\text{N}$ -labelled hexasaccharide ( $\text{HA}_6$ ) were monitored using 2-dimensional [ $^1\text{H}$ - $^{15}\text{N}$ ] HSQC spectra, which allowed the apparent  $\text{p}K_{\text{a}}$ s of the interior amides (i.e.,  $\gamma\text{HN}$  and  $\omega\text{HN}$ ) to be measured individually (Figure 2B, C); the fitted curves for  $^1\text{H}$  nuclei are shown in Figure 4. As found in the shorter oligomers, the  $\text{p}K_{\text{a}}$  observed at each interior position in  $\text{HA}_6$  was indistinguishable from that of 2,3,4-trimethoxyl-GlcA (Table 1) and the magnitude of chemical shift perturbation is less than 250 ppb, indicating that in the centre of this longer oligomer there is still no evidence for a significantly populated transient amide-carboxylate hydrogen bond or stably-bound water molecule. This is in sharp contrast to the large perturbation ( $\sim 1.5$  ppm) seen for amide groups (in  $\text{HA}_6$ ) in DMSO solution, which make highly populated intramolecular amide-carboxylate hydrogen bonds [17]. During the titration of  $\text{HA}_6$ , the  $\gamma\text{HN}$  group was observed to split progressively into two distinct resonances, reaching a maximum separation at  $\text{pH} \approx 3$  (i.e., coincident with the  $\text{p}K_{\text{a}}$ ; Figure 2B, 2C), but then recombining at pH values distant from the  $\text{p}K_{\text{a}}$  (see points at pH 1.4 and 6.1 in Figure 2B). The height ratio of these two peaks corresponds to that of the  $\alpha$ - and  $\beta$ -anomers and therefore probably reflects a small difference ( $< 0.1$  unit) in  $\text{p}K_{\text{a}}$  of the carboxylate group adjacent to the reducing terminal  $\alpha$ - and  $\beta$ -anomer rings (the peaks have been labelled accordingly, i.e.,  $\gamma^{\alpha}\text{HN}$ ,  $\gamma^{\beta}\text{HN}$ ). A similar behaviour was seen in the  $\omega\text{HN}$  group of  $\text{HA}_4$  at the  $\text{p}K_{\text{a}}$  ( $\omega^{\alpha}\text{HN}$ ,  $\omega^{\beta}\text{HN}$ ; Figure 2D).

The  $pK_a$  measured on high molecular weight HA ( $2.9 \pm 0.1$  [31]) is also not significantly different from free 2,3,4-trimethoxyl-GlcA (3.03) or that seen in the oligomers (mean value:  $2.98 \pm 0.09$ ). The magnitude of chemical shift perturbation ( $\sim 100$  ppb) is significantly less than 250 ppb and similar to that of the oligomers (100 ppb – 140 ppb). It is therefore concluded that the amide groups in the polymer are also not forming significantly populated intramolecular hydrogen bonds to carboxylate groups or trapping water molecules in stable bridges, refuting both the TF-INTRA and TF-WB models for the secondary structure. This result is also incompatible with the presence of the intermolecular amide-carboxylate hydrogen bonds required by the TF-INTER-S tertiary structure models, which have one such hydrogen bond per disaccharide unit [21, 22, 24, 25].

*Amide proton chemical shift is inconsistent with amide-carboxylate hydrogen bonds*

One dimensional NMR spectra of hyaluronan chains of various lengths were recorded in the presence and absence of physiological NaCl concentrations (150 mM) at pH values above (pH 6.0) and below (pH 1.4) the  $pK_a$  (2.98) of the GlcA carboxylate group (Figure 5). In the case of HA<sub>4</sub> and HA<sub>8</sub> (the octasaccharide), no differences in <sup>1</sup>H chemical shift were seen at any amide proton at either pH 6.0 or 1.4 upon the addition of 150 mM NaCl, indicating that these monovalent ions have no direct involvement in the secondary structure, consistent with previous reports on HA<sub>4</sub> and HA<sub>6</sub> [11, 13, 32]. Spectra recorded on HA<sub>40</sub>, a length that has been reported to dimerise and form hairpin structures [33], also revealed that the interior amide protons have no difference in chemical shift from HA<sub>8</sub> at either pH extreme (Figure 5) or in the presence of NaCl. Such structures would be expected to induce widespread chemical shift perturbations at the amide protons, which are quite sensitive to subtle variations in structure [5] and therefore, since the resonances are not perturbed and no secondary resonances from minor conformations appear, it is concluded that such associations can only be present at very low abundance (i.e., involving < 2% of amide groups). Turning to spectra of high molecular weight HA in conditions in which tertiary structures have been reported to be formed [21], there is still no perturbation to the amide chemical shift at high or low pH or with NaCl relative to the oligomers. Since in the oligomers this chemical shift indicates the lack of amide-carboxylate hydrogen bonds (as detailed above), these data are incompatible with the TF-INTER-S tertiary structure models, which require a very high proportion of amide protons in the polymer to be involved in such hydrogen bond interactions between HA chains [21, 22, 24, 25]. This conclusion is further supported by the apparent similarity of

linewidth of HA<sub>40</sub> and the polymer, which suggests there is no significant change in the local chain dynamics between these lengths.

*[<sup>1</sup>H-<sup>1</sup>H-<sup>15</sup>N] NOESY-HSQC spectrum of HA<sub>8</sub> is inconsistent with a two-fold helical geometry*

A [<sup>1</sup>H-<sup>1</sup>H-<sup>15</sup>N] NOESY-HSQC spectrum (Figure 6) was recorded on a sample of <sup>15</sup>N-labelled HA<sub>8</sub>, allowing the resolution of NOEs to each HN group within the molecule (i.e., within each disaccharide unit). This is the first determination of non-overlapping [<sup>1</sup>H-<sup>1</sup>H] NOEs at specific positions within an HA octasaccharide and therefore provides unique insight into the chain helical conformation along the length of the molecule. Moreover, the  $\psi$  position can be used to assess the conformation of the polymer in solution, since it experiences only minimal end-effects [5].

As the distance to the centre of the HA<sub>8</sub> molecule decreases (from  $\beta$  to  $\omega$  to  $\gamma$  to  $\psi$ ), the overall NOE intensity progressively increases in each strip, consistent with a relative decrease in overall local mobility (i.e., the middle ‘flexes’ less than the ends), as observed previously in HA<sub>6</sub> [26, 34]. In addition to this trend, the order of intensities of each NOE is constant throughout the molecule ( $H^3 > \text{GlcA } H^1 > H^1 > H^2$ ), i.e., the local geometry is very similar at all positions. The fact that the NOE from  $H^2$  is considerably weaker than  $H^1$  or  $H^3$  shows that the *N*-acetyl sidechain is in a basically *trans* conformation at all positions (i.e., inconsistent with the TF-INTRA model). Furthermore, these data are incompatible with an extended two-fold helical conformation for HA oligosaccharides, since in such a conformation the GlcNAc  $H^N$  proton should be considerably closer to the GlcNAc  $H^1$  proton than the GlcA  $H^1$  proton ( $H^N - \text{GlcNAc } H^1$  distance = 2.5 Å;  $H^N - \text{GlcA } H^1$  distance = 4.1 Å [16]) but these NOE data indicate the opposite throughout the molecule ( $H^N - \text{GlcNAc } H^1$  distance  $>$   $H^N - \text{GlcA } H^1$  distance). Since the  $\psi$  resonance in HA<sub>8</sub> is representative of the polymer interior [5], it is also concluded that the TF-INTER-S tertiary structure model, which necessitate an extended two-fold helical conformation for polymeric HA in solution [21, 22, 24, 25], is irreconcilable with these data.

*[<sup>1</sup>H-<sup>15</sup>N] NOE enhancement at different pH values is inconsistent with amide-carboxylate hydrogen bonds*

Previously we have measured the [<sup>1</sup>H-<sup>15</sup>N] heteronuclear NOE enhancement ( $\eta$ ) at pH 6.0 at each GlcNAc ring within HA oligomers up to HA<sub>8</sub>, and used the determined values to calculate the extent of libration (i.e., oscillation about the mean position) of each *N*-acetyl

sidechain [26]. If the amide group is somewhat tethered to the carboxylate group by an intramolecular hydrogen bond (TF-INTRA model) or tightly bound water-bridge (TF-WB model), it would be expected that protonation of the carboxylate group would result in a change in the interaction network, which would manifest as a change in the extent of libration. Therefore, the  $\eta$  value was determined at pH 1.4 for all resolvable amide groups within HA<sub>4</sub>, HA<sub>6</sub> and HA<sub>8</sub> (Table 2). In the case of the internal amide groups, the  $\eta$  values at pH 6.0 and pH 1.4 were not found to be significantly different (ratio = 1.0 within error), indicating that a change in ionisation state in fact does not noticeably alter the interaction network around the amide group. However, it could be proposed that this is because the experiment is not sensitive enough to detect such a change in interaction network with pH. In response to this, it is noted that the  $\alpha$ -anomer amide position, which is not expected to be involved in any intramolecular hydrogen-bonding interaction that could change with pH, is significantly less dynamic at low pH. The exact cause of this difference cannot be ascertained from these data, but it is reasonable to propose it arises from subtle changes in local water structure.

*Amide group  $^3J_{HH}$  coupling constants are inconsistent with amide-carboxylate hydrogen bonds*

The magnitude of the  $^3J_{HH}$  coupling constant between the H<sup>N</sup> and H<sup>2</sup> protons is related to the *N*-acetyl sidechain conformation. Unfortunately, no precise Karplus equation exists for this particular group in HA, and it has therefore been debated whether values previously measured in aqueous solution correspond to *cis* or *trans* conformations or an interchanging mixture of both [15, 19]. However, the [<sup>1</sup>H-<sup>1</sup>H] NOE data presented here show that the high values of  $^3J_{HH}$  typically seen in water do indicate an orientation that is on average *trans*. Complementing previous studies [12], we have measured the  $^3J_{HH}$  coupling constant at pH values either side of the carboxylate p*K*<sub>a</sub> in oligomers of different lengths (Table 3) to a greater precision ( $\pm 0.2$  Hz). The coupling was determined to be 9.8 - 9.9  $\pm$  0.2 Hz at the interior positions of the oligomers studied at both pH 6.0 and 1.4, indicating that change of the ionization state of the carboxylate group has negligible effect on the orientation and/or libration of the *N*-acetyl sidechain (as was concluded from the [<sup>1</sup>H-<sup>15</sup>N]-NOE data, and also at odds with the TF-INTRA and TF-WB models). The addition of NaCl was found to make no appreciable difference, consistent with the lack of perturbation to the amide chemical shift in the 1D spectra (see above). No  $^3J_{HH}$  coupling was seen to vary with temperature (10 - 35 °C),

as was found for the reducing terminal positions of the disaccharide GlcA-GlcNAc~OH [11]. It was not possible to measure the  $^3J_{\text{HH}}$  in HA<sub>40</sub> or the polymer because of the line-broadening. However, since the interior amide chemical shift is no different to that of the octamer (Figure 5), there is no reason to suppose the *N*-acetyl sidechains assume another average conformation.

*Temperature coefficients of amide protons are inconsistent with amide-carboxylate hydrogen bonds*

Temperature coefficients of protons ( $\Delta\delta/\Delta T$ ) involved in hydrogen bonds are expected to be smaller than those that are freely exchanging with water ( $\sim 11$  ppb/K). In proteins, 85 % of amide protons with temperature coefficients ( $\Delta\delta_{\text{HN}}/\Delta T$ ) less negative than  $-4.6$  ppb/K are involved in hydrogen bonds (to carbonyl groups) [35, 36]. In oligosaccharides in DMSO, hydroxyl proton temperature coefficients  $> -3$  ppb/K are expected for strong hydrogen bonds [37]. In HA oligomers in DMSO, the interior amide protons report  $\Delta\delta_{\text{HN}}/\Delta T$  coefficients of  $-4.3$  ppb/K, indicating that they make a medium-strength hydrogen bond to the carboxylate group [17]. Temperature coefficients generally only change with pH when they are associated with concomitant conformational changes [35]. Measurement of temperature coefficients in HA should therefore provide information for evaluation of the secondary and tertiary structure models.

Chemical shifts of amide protons were measured at 15, 25 and 35 °C for various HA lengths at pH 6.0 and 1.4 (Supplementary Table 2), and in all cases a straight line fit was possible (coefficient of determination,  $R^2$ ,  $> 0.99$ ), consistent with earlier reports that temperature does not affect the conformation of HA oligomers [11]. The  $\alpha\text{H}^{\text{N}}$  and  $\beta\text{H}^{\text{N}}$   $\Delta\delta/\Delta T$  values observed (Table 4) are indistinguishable from those of GlcNAc ( $\sim 9.0$  ppb/K and  $\sim 7.7$  ppb/K, respectively), irrespective of oligomer length, pH and the presence of physiological NaCl. Since the GlcNAc acetamido group is interacting purely with water in both  $\alpha$  and  $\beta$  anomers, these values indicate that the  $\alpha$  and  $\beta$  acetamido groups in HA oligosaccharides are not making intramolecular hydrogen bonds (as would be expected) or significantly different interactions with water molecules from those found in GlcNAc. All interior amide protons report a  $\Delta\delta_{\text{HN}}/\Delta T$  of  $\sim 6.7$  ppb/K at pH 6.0, which changes to  $\sim 8.0$  ppb/K at pH 1.4. Since these values are considerably more negative than the cut-off detailed above, it is clear that the interior amide groups do not make hydrogen bonds with the carboxylate group in either its

protonated or charged state, or stably-bound water bridges (i.e., refuting the TF-INTRA and TF-WB models). These values are unaffected by the length of HA chain and the presence of physiological NaCl, and remain the same in conditions of chain length, pH and NaCl concentration under which the tertiary structures [21, 22, 24, 25] have been reported to form (i.e., HA<sub>2500-8000</sub> + NaCl in Table 4). Therefore, the TF-INTER-S tertiary structure models, which propose that the majority of amide groups contribute to the chain-chain associations by intermolecular hydrogen bonds, are incompatible with these data.

*Amide exchange rates are inconsistent with amide-carboxylate hydrogen bonds*

Hydrogen bonds can be assessed by measuring the exchange-rate of protons with solvent, with those displaying half-lives longer than several minutes being candidates for protection by hydrogen bonding. In the case of HA<sub>6</sub>, half-lives of the amide protons in aqueous solution have been determined to be 500 ms ( $\gamma\text{H}^{\text{N}}$ ,  $\omega\text{H}^{\text{N}}$ ), 200 ms ( $\alpha\text{H}^{\text{N}}$ ) and 60 ms ( $\beta\text{H}^{\text{N}}$ ) (i.e., all in fast-exchange) [18], indicating that they should not be considered to be involved in stable hydrogen bond interactions (the pH at which these measurements were taken was not specified, although examination of the spectra indicates it was above pH 5). Normalised exchange build-up curves for each amide position within HA<sub>4</sub> and HA<sub>6</sub> at pH 6.0 were generated (Figure 7), and the relative half-lives determined from these data are consistent with those measured previously [18] (i.e.,  $\beta\text{H}^{\text{N}}$  and  $\alpha\text{H}^{\text{N}}$  exchange ~13 and ~3.5 times faster than the interior positions, for both HA<sub>4</sub> and HA<sub>6</sub>). While it is clear that there is a significant difference in exchange rate between the  $\beta$  and  $\omega$  positions, there is only a factor of 2.5 - 3.5 between  $\alpha$  and  $\omega$  positions, suggesting that the variations are more likely to reflect differences in local solvent accessibility and interactions with water molecules than the loss of a hydrogen bond network involving the carboxylate group.

## Discussion

Three different hydrogen bond arrangements between the amide hydrogen and carboxylate groups are commonly proposed to exist in HA in aqueous solution (intramolecular, water-bridged and intermolecular), although there is much controversy over their strength, persistence times and frequency of formation. The data presented here show that there are no highly populated hydrogen bonds or stably-bound water molecules between amide and carboxylate groups in HA in aqueous physiological solution, invalidating a crucial aspect of

some models for the secondary (i.e., TF-INTRA, TF-WB) and tertiary (i.e., TF-INTER) conformations.

In oligomers, the amide proton is close enough to report the change in electric field of adjacent carboxylate groups upon titration, but the lack of suppression of the  $pK_a$  value, magnitude of chemical shift perturbation, temperature coefficient and solvent exchange rates are incompatible with the presence of an abundant (>20 % populated) transient hydrogen bond between the groups. While it is entirely possible that the small chemical shift perturbation of the amide protons (100 – 140 ppb) upon titration of the adjacent carboxylate is solely due to changes in the local electrostatic field, it may also result in part from very low abundance conformations (5 – 10 %) of the HA chain that make transient intramolecular hydrogen bonds. This would be consistent with the DYN models that suggest that the HA chain rapidly interconverts between various helical conformations in solution, some of which make such direct interactions [38]. It is to be noted that the secondary structure models for other glycosaminoglycans [9, 39, 40], which were derived in the same manner as that of HA, may therefore also be flawed.

Nevertheless, differences in temperature coefficients and the slightly retarded rate of solvent exchange rate between interior and end groups indicate that the adjacent GlcA ring is having some effect on interior amide groups. Since these properties are directly related to the chemical exchange of these protons with water, such differences mostly likely reflect subtle variations in solvent accessibility between the interior and end groups. The simplest explanation is steric exclusion of water by the adjacent bulky carboxylate group, but it is also entirely consistent with these data that interior amide groups could be slightly protected from solvent exchange by the formation of transient water-bridges and (sparsely populated) hydrogen bonds between amide and carboxylate groups, as suggested in the DYN model [7, 14, 15].

The change in  $\Delta\delta_{\text{HN}}/\Delta T$  with pH was the only experiment performed that sensed a discernible alteration in the amide-carboxylate relationship; also recorded here are the temperature coefficients of the associated  $^{15}\text{N}$  nuclei ( $\Delta\delta_{15\text{N}}/\Delta T$ , Table 4) that report the same phenomenon but with greater sensitivity. Unfortunately, while the measured values are reproducibly constant under a range of conditions, an explanation of the change with pH is not possible at

present (in the case of the  $\Delta\delta_{15N}/\Delta T$  values, we know of no previous reports of such parameters). Nevertheless, it is reasonable to propose that the temperature coefficient perturbation originates from subtle changes in the carboxylate group's local structure and/or solvation having some effect on the solvent accessibility of the interior amide protons.

Polymeric HA (0.5 – 1.5 MDa = HA<sub>2500-8000</sub>) has been studied in this work under conditions (2 mg/ml, 150 mM NaCl) similar to those reported to form tertiary structures in solution (1 MDa, 10 mg/ml, 290 mM NaCl [21]; 0.4 – 4.0 MDa, 1 $\mu$ g/ml – 1mg/ml, 0.5 M NH<sub>4</sub>CH<sub>3</sub>COO [24]; 1 MDa, 10 mg/ml, 150 mM NaCl [22]). These structures are hypothesised to be vast stable honeycombed networks of intertwined HA chains [21], which would be expected to be invisible to NMR in aqueous solution due to the extremely broad line widths arising from the high molecular weight and ensuing long correlation times, i.e., any remaining non-broad resonances seen would be expected to arise from saccharides not involved in the meshwork. Crucially, the changes in line-width with molecular size (and chemical modification) that the tertiary structure models are based on have been measured on these same visible saccharides [21, 22]. Therefore, if this is the case, the data measured on them could not be used to support the TF-INTER-S tertiary structure model. However, it could be supposed that the tertiary structures are in a process of rapid formation and remodelling, or that they maintain extremely high local dynamic motion, making them NMR-visible. Supposing this hypothesis may be true, the resonances observed from high molecular weight HA in solution were examined to see if they are consistent with the TF-INTER-S tertiary structure models.

The <sup>1</sup>H chemical shift of the interior amide protons in high molecular weight HA is indistinguishable from that of HA<sub>8</sub>, showing that there are no significant differences in the amide proton environment between the centre of octasaccharides and the polymer. In addition, the GlcA pK<sub>a</sub> value, amide proton chemical shift perturbations and temperature coefficients, in a range of conditions, are identical to that of oligosaccharides. Since these properties are conclusive for the lack of stable intramolecular hydrogen bonds between amide and carboxylate groups in the HA oligomers, it is clear that at high molecular weight there are also no such interactions present in the secondary structure. Moreover, these data are irreconcilable with a transition to tertiary structures involving the formation of strong intermolecular hydrogen bonds by a high proportion of the amide groups.

Another crucial feature of the TF-INTER-S tertiary structure models is the association of hydrophobic patches on alternate HA chains, which requires an extended two-fold helical conformation for the HA chains. However, clearly resolved NOEs from the centre of HA<sub>8</sub> show that the chain does not adopt an extended two-fold helical conformation. Since there are no discernible differences in the properties of the amide group between the centre of octasaccharides and the polymer, it is concluded that there is no reason to believe that the conformation of the polymer changes to that of an extended two-fold helix. This is consistent with <sup>13</sup>C chemical shifts, which are sensitive to changes in the average glycosidic torsional angles [13, 23], that have a total absence of perturbations between the centre of oligomers and the polymer [13, 21]. This lack of <sup>13</sup>C chemical shift perturbations is even more troubling for the tertiary structure models because the stacking of hydrophobic patches would be expected to induce large chemical shift perturbations in the C-H groups involved. Rather, these NMR studies indicate there is no significant association of HA chains at physiological NaCl and pH conditions, in agreement with hydrodynamic data. Nevertheless, it remains a possibility from these NMR data that there are transient and low-abundance (and possibly non-specific) chain-chain interactions involving < 2% of disaccharide units at any particular moment [6, 41].

It is worth reiterating that the only experimental evidence for extended two-fold helical conformations of HA comes from fibre-diffraction patterns of the acid form of HA, which could not be indexed because of its poor quality [42]. While these diffraction data are consistent with a two-fold helix, they are not prescriptive for one. However, these data were used to construct the extended two-fold helical model of HA [16]. This speculative model conformation of the acid form of dried-fibre HA was then used, in combination with data from studies in DMSO [18, 43], to construct both secondary (TF-INTRA, TF-WB) and tertiary (TF-INTER-S) models of the aqueous solution conformation at physiological pH [24, 25]. The applicability of molecular descriptions based on unsolved diffraction data at pH ~2 to physiological pH conditions is questionable, especially since HA becomes fully protonated at pH 2 and therefore would be expected to have significant differences in its physical properties. It should further be noted that the diagram detailing the hydrophobic patch stacking interactions is incorrect: the middle molecule in the two figures presented (1B in [21] and 1B,1C in [22]) has different hydrophobic patches from the upper and lower molecules, whereas they should be identical (as in our Figure 1D). This actually means the extent of hydrophobic patch overlap is not two full and one half-hydrophobic faces (per disaccharide) as implied by these diagrams, but a mere two half-hydrophobic faces. In addition, there is one

full and two half-hydrophilic faces stacking against hydrophobic areas. Since there are in fact more unfavourable stacking interactions than favourable ones, we conclude that there is no sound theoretical basis for HA chains hydrophobically stacking in the manner proposed. This should not be taken to imply that the hydrophobic patch is not otherwise important in hyaluronan biology, as evidenced by its crucial role in interactions with proteins [44].

The relatively broad  $^{13}\text{C}$  carbonyl resonance of high molecular weight HA, which was used to support the TF-INTER-S tertiary structure models [21-23], needs further experimental investigation before an atomistic explanation can be attempted. Since the chemical shift is only broadened and not perturbed, it is unlikely that the broadening arises from exchange between two different chain conformations (which would be expected to have different chemical shifts) especially since no other  $^{13}\text{C}$  chemical shifts are perturbed or broadened throughout the molecule [13, 21]. Rather, the broadening of this resonance is more likely to arise from a particular relaxation mechanism (e.g. of the methyl group) that is selected for by the different correlation time present in the larger molecules (and differences in anisotropic motions). In this regard, shearing causes the resonance to broaden further as the chain becomes extended and mobility is reduced [23], while an increase in temperature, which would be expected to enhance chain mobility, results in sharpening of the resonance [22]. This change with temperature is particularly noteworthy since the amide proton, which is in the same rigid peptide unit as the carbonyl carbon atom, does not show any change in linewidth over the same temperature range [22] although the changes in the carbonyl resonance linewidth were used to support the tertiary structure models [22].

The observed identity of NMR parameters between the centre of octasaccharides and polymeric HA means that it is reasonable to transfer measurements of the local geometry and dynamics in the centre of octasaccharides into new descriptions for the polymer. In essence, the NMR data from polymeric HA in physiological solution indicate that structuring occurs only at the level of rapidly interchanging hydrogen bond arrangements between hydroxyl groups and water molecules across adjacent saccharide rings. Therefore, multiple repetitions of these properties into new models of the polymer should provide new atomistic accounts for the solution properties of high molecular-mass HA. In addition, comparison of the parameters measured on HA in this work to other glycosaminoglycans will provide new insights into the consequences of the subtle differences in linkage and residue structure within the family, and their biological ramifications.

## Acknowledgements

This work was funded by a Biotechnology and Biological Sciences Research Council Sir David Phillips research fellowship. PLD was supported by the National Science Foundation MCB-9876193. NMR data was recorded on Oxford Centre for Molecular Sciences spectrometers (University of Oxford, UK) under the support of Prof. Iain D. Campbell.

## Abbreviations

DMSO, dimethyl sulphoxide; DYN, dynamic model for secondary structure; GlcA, D-glucuronic acid; GlcNAc, *N*-acetyl-D-glucosamine; HA, hyaluronan; HSQC, heteronuclear single quantum correlation; TF-INTRA, secondary structure model involving an extended two-fold helical conformation and intramolecular hydrogen bonds; TF-WB, secondary structure model involving an extended two-fold helical conformation and stably-bound bridging water molecules; TF-INTER-S, tertiary structure model involving an extended two-fold helical conformation, intermolecular hydrogen bonds and hydrophobic stacking interactions.

## References

- 1 Termeer, C. C., Hennies, J., Voith, U., Ahrens, T., Weiss, J. M., Prehm, P. and Simon, J. C. (2000) Oligosaccharides of hyaluronan are potent activators of dendritic cells. *J. Immunol.* **165**, 1863-70
- 2 Moseley, R., Waddington, R. J. and Embery, G. (1997) Degradation of glycosaminoglycans by reactive oxygen species derived from stimulated polymorphonuclear leukocytes. *Biochim. Biophys. Acta* **1362**, 221-31
- 3 Hascall, V. C. and Heinegard, D. (1974) Aggregation of cartilage proteoglycans. I. The role of hyaluronic acid. *J. Biol. Chem.* **249**, 4232-41
- 4 Richards, J. S. (2005) Ovulation: New factors that prepare the oocyte for fertilization. *Mol. Cell. Endocrinol.* **234**, 75-9
- 5 Blundell, C. D., DeAngelis, P. L., Day, A. J. and Almond, A. (2004) Use of <sup>15</sup>N-NMR to resolve molecular details in isotopically-enriched carbohydrates: sequence-specific observations in hyaluronan oligomers up to decasaccharides. *Glycobiology* **14**, 999-1009
- 6 Cowman, M. K., Spagnoli, C., Kudasheva, D., Li, M., Dyal, A., Kanai, S. and Balazs, E. A. (2005) Extended, relaxed, and condensed conformations of hyaluronan observed by atomic force microscopy. *Biophys. J.* **88**, 590-602
- 7 Cowman, M. K. and Matsuoka, S. (2005) Experimental approaches to hyaluronan structure. *Carbohydr. Res.* **340**, 791-809
- 8 Scott, J. E., Heatley, F., Moorcroft, D. and Olavesen, A. H. (1981) Secondary structures of hyaluronate and chondroitin sulphates. *Biochem. J.* **199**, 829-832
- 9 Scott, J. E. and Tigwell, M. J. (1978) Periodate oxidation and the shapes of glycosaminoglycuronans in solution. *Biochem. J.* **173**, 103-114

- 10 Toffanin, R., Kvam, B. J., Flaibani, A., Atzori, M., Biviano, F. and Paoletti, S. (1993) NMR studies of oligosaccharides derived from hyaluronate: complete assignment of  $^1\text{H}$  and  $^{13}\text{C}$  NMR spectra of aqueous di- and tetra-saccharides, and comparison of chemical shifts for oligosaccharides of increasing degree of polymerisation. *Carbohydr. Res.* **245**, 113-28
- 11 Sicinska, W., Adams, B. and Lerner, L. (1993) A detailed  $^1\text{H}$  and  $^{13}\text{C}$  NMR study of a repeating disaccharide of hyaluronan: the effects of temperature and counterion type. *Carbohydr. Res.* **242**, 29-51
- 12 Cowman, M. K., Cozart, D., Nakanishi, K. and Balazs, E. A. (1984)  $^1\text{H}$  NMR of glycosaminoglycans and hyaluronic acid oligosaccharides in aqueous solution: the amide proton environment. *Arch. Biochem. Biophys.* **230**, 203-12
- 13 Cowman, M., Hittner, D. and Feder-Davis, J. (1996)  $^{13}\text{C}$ -NMR studies of hyaluronan: conformational sensitivity to varied environments. *Macromolecules* **29**, 2894-2902
- 14 Kaufmann, J., Möhle, K., Hofman, J.-G. and Arnold, K. (1998) Molecular dynamics study of hyaluronic acid in water. *J. Mol. Struct.* **422**, 109-121
- 15 Almond, A., Brass, A. and Sheehan, J. K. (1998) Dynamic exchange between stabilised conformations predicted for hyaluronan tetrasaccharides: comparison of molecular dynamics simulations with available NMR data. *Glycobiology* **8**, 973-980
- 16 Atkins, E. D. T., Meader, D. and Scott, J. E. (1980) Model of hyaluronic acid incorporating four hydrogen bonds. *Int. J. Biol. Macromol.* **2**, 318-319
- 17 Scott, J. E., Heatley, F. and Hull, W. E. (1984) Secondary structure of hyaluronate in solution. A  $^1\text{H}$ -n.m.r. investigation at 300 and 500 MHz in  $[\text{}^2\text{H}_6]$ dimethyl sulphoxide solution. *Biochem. J.* **220**, 197-205.
- 18 Heatley, F. and Scott, J. E. (1988) A water molecule participates in the secondary structure of hyaluronan. *Biochem. J.* **254**, 489-93
- 19 Holmbeck, S. M. A., Petillo, P. A. and Lerner, L. E. (1994) The solution conformation of hyaluronan: a combined NMR and molecular dynamics study. *Biochemistry* **33**, 14246-14255
- 20 Day, A. J. and Sheehan, J. K. (2001) Hyaluronan: polysaccharide chaos to protein organisation. *Curr. Opin. Struct. Biol.* **11**, 617-22.
- 21 Scott, J. E. and Heatley, F. (1999) Hyaluronan forms specific stable tertiary structures in aqueous solution: a  $^{13}\text{C}$  NMR study. *Proc. Natl. Acad. Sci. U. S. A.* **96**, 4850-5
- 22 Scott, J. E. and Heatley, F. (2002) Biological properties of hyaluronan in aqueous solution are controlled and sequestered by reversible tertiary structures, defined by NMR spectroscopy. *Biomacromolecules* **3**, 547-53
- 23 Fischer, E., Callaghan, P. T., Heatley, F. and Scott, J. E. (2002) Shear flow affects secondary and tertiary structures in hyaluronan solution as shown by rheo-NMR. *J. Mol. Struct.* **602**, 303-311
- 24 Scott, J. E., Cummings, C., Brass, A. and Chen, Y. (1991) Secondary and tertiary structures of hyaluronan in aqueous solution, investigated by rotary shadowing-electron microscopy and computer simulation. Hyaluronan is a very efficient network-forming polymer. *Biochem. J.* **274**, 699-705
- 25 Mikelsaar, R. H. and Scott, J. E. (1994) Molecular modelling of secondary and tertiary structures of hyaluronan, compared with electron microscopy and NMR data. Possible sheets and tubular structures in aqueous solution. *Glycoconj. J.* **11**, 65-71
- 26 Almond, A., DeAngelis, P. L. and Blundell, C. D. (2005) Dynamics of hyaluronan oligosaccharides revealed by  $^{15}\text{N}$  relaxation. *J. Am. Chem. Soc.* **127**, 1086-7
- 27 Seyfried, N. T., Blundell, C. D., Day, A. J. and Almond, A. (2005) Preparation and application of biologically active fluorescent hyaluronan oligosaccharides. *Glycobiology* **15**, 303-12

- 28 Mahoney, D. J., Aplin, R. T., Calabro, A., Hascall, V. C. and Day, A. J. (2001) Novel methods for the preparation and characterization of hyaluronan oligosaccharides of defined length. *Glycobiology* **11**, 1025-33
- 29 Haruyama, H., Qian, Y. Q. and Wuthrich, K. (1989) Static and transient hydrogen-bonding interactions in recombinant desulfatohirudin studied by  $^1\text{H}$  nuclear magnetic resonance measurements of amide proton exchange rates and pH-dependent chemical shifts. *Biochemistry* **28**, 4312-7
- 30 Szyperski, T., Antuch, W., Schick, M., Betz, A., Stone, S. R. and Wuthrich, K. (1994) Transient hydrogen bonds identified on the surface of the NMR solution structure of Hirudin. *Biochemistry* **33**, 9303-10
- 31 Cleland, R. L., Wang, J. L. and Detweiler, D. M. (1982) Polyelectrolyte properties of sodium hyaluronate. 2. Potentiometric titration of hyaluronic acid. *Macromolecules* **15**, 386-395
- 32 Sicinska, W. and Lerner, L. E. (1996) A detailed  $^1\text{H}$  and  $^{13}\text{C}$  NMR study of a repeating disaccharide of hyaluronan: the effect of sodium and calcium ions. *Carbohydr. Res.* **286**, 151-9
- 33 Turner, R. E., Lin, P. Y. and Cowman, M. K. (1988) Self-association of hyaluronate segments in aqueous NaCl solution. *Arch. Biochem. Biophys.* **265**, 484-95
- 34 Cowman, M. K., Feder-Davis, J. and Hittner, D. M. (2001)  $^{13}\text{C}$  NMR studies of hyaluronan. 2. Dependence of conformational dynamics on chain length and solvent. *Macromolecules* **34**, 110-115
- 35 Cierpicki, T. and Otlewski, J. (2001) Amide proton temperature coefficients as hydrogen bond indicators in proteins. *J. Biomol. NMR.* **21**, 249-61
- 36 Baxter, N. J. and Williamson, M. P. (1997) Temperature dependence of  $^1\text{H}$  chemical shifts in proteins. *J. Biomol. NMR.* **9**, 359-69
- 37 Poppe, L., Stuike-Prill, R., Meyer, B. and van Halbeek, H. (1992) The solution conformation of sialyl- $\alpha$  (2----6)-lactose studied by modern NMR techniques and Monte Carlo simulations. *J. Biomol. NMR* **2**, 109-36
- 38 Almond, A., Brass, A. and Sheehan, J. K. (1998) Deducing polymeric structure from aqueous molecular dynamics simulations of oligosaccharides: predictions from simulations of hyaluronan tetrasaccharides compared with hydrodynamic and X-ray fibre diffraction data. *J. Mol. Biol.* **284**, 1425-37
- 39 Scott, J. E., Heatley, F., Moorcroft, D. and Olavesen, A. H. (1981) Secondary structures of hyaluronate and chondroitin sulphates. A  $^1\text{H}$  n.m.r. study of NH signals in dimethyl sulphoxide solution. *Biochem. J.* **199**, 829-32
- 40 Scott, J. E., Heatley, F. and Wood, B. (1995) Comparison of secondary structures in water of chondroitin-4-sulfate and dermatan sulfate: implications in the formation of tertiary structures. *Biochemistry* **34**, 15467-74
- 41 Gribbon, P., Heng, B. C. and Hardingham, T. E. (2000) The analysis of intermolecular interactions in concentrated hyaluronan solutions suggest no evidence for chain-chain association. *Biochem. J.* **350**, 329-35
- 42 Atkins, E. D., Phelps, C. F. and Sheehan, J. K. (1972) The conformation of the mucopolysaccharides. Hyaluronates. *Biochem. J.* **128**, 1255-63
- 43 Heatley, F., Scott, J. E., Jeanloz, R. W. and Walker-Nasir, E. (1982) Secondary structure in glycosaminoglycuronans: N.M.R. spectra in dimethyl sulphoxide of disaccharides related to hyaluronic acid and chondroitin sulphate. *Carbohydr. Res.* **99**, 1-11
- 44 Blundell, C. D., Almond, A., Mahoney, D. J., DeAngelis, P. L., Campbell, I. D. and Day, A. J. (2005) Towards a structure for a TSG-6.hyaluronan complex by modeling

and NMR spectroscopy: insights into other members of the link module superfamily.  
J. Biol. Chem. **280**, 18189-201

**Tables**
**Table 1. Observed  $pK_a$  values of selected HA saccharides**

Saccharide	Observed $pK_a^a$ at reporter position:				chemical shift change ( $\Delta\delta$ ) on protonation /ppb <sup>b,c</sup>			
	HN $\beta$	HN $\alpha$	HN $\omega$	HN $\gamma$	HN $\beta$	HN $\alpha$	HN $\omega$	HN $\gamma$
HA <sub>3</sub> <sup>NN</sup>	3.0	3.0	2.8		21	15	-140	
$\Delta$ -HA <sub>4</sub>	2.9	2.9	2.9/3.1 <sup>c</sup>		21	20	-124	
HA <sub>4</sub>	3.0	3.0	2.9		22	21	-109	
<sup>15</sup> N-HA <sub>4</sub> , H <sup>N</sup> N <sup>H</sup>	2.9	3.0	2.9/2.8 <sup>d</sup>		21	20	-110/-110 <sup>d</sup>	
	3.0	3.1	2.9/3.0 <sup>d</sup>		338	222	794/779 <sup>d</sup>	
<sup>15</sup> N-HA <sub>6</sub> H <sup>N</sup> N <sup>H</sup>	3.0	3.1	3.0	3.0/2.9 <sup>e</sup>	25	25	-111	-101/-101 <sup>e</sup>
	3.1	3.2	3.1	3.0/2.9 <sup>e</sup>	352	230	722	688/673 <sup>e</sup>
HA polymer				2.9 <sup>f</sup>				-100 <sup>g</sup>

<sup>a</sup>All  $pK_a$  values measured in this work have an error of  $\pm 0.1$  units. <sup>b</sup>ppb = parts per billion. <sup>c</sup>All  $\Delta\delta$  values have an error of  $\pm 3$  ppb. <sup>d</sup> $pK_a$  values measured from the  $\omega$ H<sup>N</sup> and vinylic protons, respectively. <sup>e</sup> $pK_a$  values of the  $\omega^\alpha$ HN and  $\omega^\beta$ HN resonances, respectively. <sup>f</sup> $pK_a$  values of the  $\gamma^\alpha$ HN and  $\gamma^\beta$ HN resonances, respectively. <sup>g</sup>Value of interior carboxylates, as reported by Cleland [31]. <sup>h</sup>Estimated based on consideration of  $\Delta\delta$  between pH 6.0 and pH 1.4 for HA of  $M_r$  0.5 -1.5  $\times 10^6$ .

**Table 2. [<sup>1</sup>H-<sup>15</sup>N] NOE enhancements ( $\eta$ ) at high and low pH in various oligosaccharides**

Amide position		pH 6.0 $\eta \pm \text{error}$		pH 1.4 $\eta \pm \text{error}$		ratio pH 6.0:1.4 $\pm \text{error}$	
<sup>15</sup> N-HA <sub>4</sub>	$\beta$	-1.23	0.02	-1.52	0.04	0.8	0.1
	$\alpha$	-1.55	0.03	-1.03	0.04	1.5	0.1
	$\omega$	-1.34	0.01	-1.61	0.04	0.8	0.1
<sup>15</sup> N-HA <sub>6</sub>	$\beta$	-0.62	0.02	-0.90	0.04	0.7	0.1
	$\alpha$	-0.87	0.03	-0.64	0.04	1.4	0.1
	$\gamma$	-0.70	0.01	-0.70	0.04	1.0	0.1
	$\omega$	-0.95	0.01	-0.87	0.04	1.1	0.1
<sup>15</sup> N-HA <sub>8</sub>	$\beta$	-0.60	0.02	-0.79	0.04	0.8	0.1
	$\alpha$	-0.73	0.03	-0.46	0.04	1.6	0.2
	$\gamma$	-0.45	0.01	- <sup>a</sup>	-	-	-
	$\psi$	-0.42	0.01	- <sup>a</sup>	-	-	-
	$\omega$	-0.83	0.01	-0.68	0.04	1.2	0.1

<sup>a</sup> $\gamma$  and  $\psi$  resonances were not resolved in the [<sup>1</sup>H-<sup>15</sup>N] NOE spectra recorded at pH 1.4.

Table 3. Observed  $^3J_{\text{HH}}$  coupling constants between  $\text{H}^{\text{N}}$  and  $\text{H}^2$  nuclei in selected saccharides

Amide position		pH 6.0 $\pm 0.2$ Hz	pH 1.4 $\pm 0.2$ Hz	difference Hz
GlcNAc	$\alpha$	8.7	8.6	0.1
	$\beta$	9.8	9.3	0.5
$\text{HA}_3^{\text{NN}}$	$\alpha$	9.6	9.6	0.0
	$\beta$	10.0	9.9	0.1
	$\omega^{\text{a}}$	9.9	10.0	-0.1
$^{15}\text{N-HA}_4$	$\alpha$	9.6	9.6	0.0
	$\beta$	9.8	9.7	0.1
	$\omega^{\text{a}}$	9.8	9.8	0.0
$\text{HA}_4 + \text{NaCl}$	$\alpha$	9.8	9.9	-0.1
	$\beta$	10.1	$^{\text{b}}$	-
	$\omega^{\text{a}}$	10.2	$^{\text{b}}$	-
$\Delta\text{-HA}_4$	$\alpha$	9.8	10.1	-0.3
	$\beta$	10.2	$^{\text{b}}$	-
	$\omega^{\text{a}}$	9.8	$^{\text{b}}$	-
$^{15}\text{N-HA}_6$	$\alpha$	9.4	9.6	-0.2
	$\beta$	9.6	9.6	0.0
	$\gamma^{\text{a}}$	9.7	9.7	0.0
	$\omega$	10.0	9.7	0.3
$^{15}\text{N-HA}_8$	$\alpha$	9.7	9.5	0.2
	$\beta$	10.1	9.6	0.0
	$\gamma^{\text{a}}$	9.8	9.7	0.1
	$\psi^{\text{c}}$	9.9	9.7	0.1
	$\omega$	9.9	9.6	0.3
Mean <sup>d</sup>	$\alpha$	9.7	9.7	0.0
	$\beta$	10.0	9.7	-0.3
	internal	9.9	9.8	0.1

<sup>a</sup> $\alpha$  and  $\beta$  variants of these resonances are not distinguishable at pH 1.4 or pH 6.0 (see text). <sup>b</sup> $\beta$  and  $\omega$  resonances overlap at pH 1.4 in 1D spectra. <sup>c</sup> $\gamma$  and  $\psi$  resonances overlap at pH 1.4 in [ $^1\text{H}$ - $^{15}\text{N}$ ] HSQC spectra. <sup>d</sup>GlcNAc omitted from mean.

Table 4. Temperature coefficients of amide hydrogen and nitrogen nuclei in selected saccharides

pH 6.0	$^1\text{H}^{\text{N}} \Delta\delta_{\text{HN}}/\Delta T \pm 0.1 \text{ ppb/K}$						$^{15}\text{N}^{\text{H}} \Delta\delta_{\text{N}}/\Delta T \pm 0.1 \text{ ppb/K}$					
	$\beta$	$\alpha$	$\omega$	$\gamma$	$\phi$	$\delta$	$\beta$	$\alpha$	$\omega$	$\gamma$	$\phi$	$\delta$
GlcNAc	-7.8	-9.0					-19.0	-21.4				
HA <sub>3</sub> <sup>NN</sup>	-7.7	-9.1	-7.1									
<sup>15</sup> N-HA <sub>4</sub>	-7.7	-9.1	-7.0				-15.3	-19.4	-16.0			
HA <sub>4</sub> + NaCl <sup>a</sup>	-7.4	-8.9	-6.8									
$\Delta$ -HA <sub>4</sub>	-7.6	-9.0	-6.9									
<sup>15</sup> N-HA <sub>5</sub> <sup>AA</sup>			-6.6	-6.5/-6.7 <sup>b</sup>					-15.2	-15.0/-15.3 <sup>b</sup>		
<sup>15</sup> N-HA <sub>6</sub>	-7.6	-9.0	-6.9	-6.9			-15.2	-19.2	-15.9	-15.4		
<sup>15</sup> N-HA <sub>8</sub>	-7.6	-9.0	-6.8	-6.8	-6.8		-15.0	-19.3	-15.9	-15.4	-15.5	
<sup>15</sup> N-HA <sub>10</sub>	-7.6	-9.1	-6.9	-6.9	-6.9	-6.9	-15.3	-19.5	-16.1	-15.6	-15.7	-15.7
HA <sub>40</sub>	-7.6	-9.1				-6.9 <sup>d</sup>						
HA <sub>40</sub> + NaCl <sup>a</sup>	-7.3	-8.7				-6.7 <sup>d</sup>						
HA <sub>2500-8000</sub>						-6.7 <sup>d</sup>						
HA <sub>2500-8000</sub> + NaCl <sup>a</sup>						-6.9 <sup>d</sup>						
pH 1.4	$\beta$	$\alpha$	$\omega$	$\gamma$	$\phi$	$\delta$	$\beta$	$\alpha$	$\omega$	$\gamma$	$\phi$	$\delta$
GlcNAc	-7.7	-8.8					-18.4	-20.8				
HA <sub>3</sub> <sup>NN</sup>	-7.7	-9.1	-8.6									
<sup>15</sup> N-HA <sub>4</sub>	-7.6	-9.0	-8.1				-16.8	-20.2	-23.7			
HA <sub>4</sub> + NaCl <sup>a</sup>	-7.4	-8.8	-8.0									
$\Delta$ -HA <sub>4</sub>	-7.5	-9.0	-8.1									
<sup>15</sup> N-HA <sub>5</sub> <sup>AA</sup>			-8.3	-8.3/-8.4 <sup>b</sup>					-23.7	-23.5/-23.5 <sup>b</sup>		
<sup>15</sup> N-HA <sub>6</sub>	-7.6	-9.0	-8.1	-8.2			-16.7	-20.0	-23.5	-22.9		
<sup>15</sup> N-HA <sub>8</sub>	-7.7	-9.1	-8.2	-8.3	-8.3		-16.8	-20.2	-23.6	-22.9	-22.9	
HA <sub>40</sub>	-7.4	-8.9				-8.0 <sup>c</sup>						
HA <sub>40</sub> + NaCl <sup>a</sup>	-7.3					-8.0 <sup>c</sup>						
HA <sub>2500-8000</sub>						-8.1 <sup>c</sup>						
HA <sub>2500-8000</sub> + NaCl <sup>a</sup>						-7.9 <sup>c</sup>						

<sup>a</sup>NaCl concentration at 150 mM. <sup>b</sup> $\alpha$  and  $\beta$  variants, respectively. <sup>c</sup>Temperature coefficient displayed by the degenerate internal amide resonances.

### Figure legends

**Figure 1.** A) Chemical structure of a hyaluronan (HA) trisaccharide, showing the relationship of *N*-acetyl-D-glucosamine (GlcNAc) residues to their adjacent D-glucuronic acid (GlcA) rings. Key hydrogen atoms relevant to this work are shown (GlcNAc H<sup>1</sup>, H<sup>2</sup>, H<sup>3</sup>; GlcA H<sup>1</sup>). The *N*-acetyl sidechain is shown in the *trans* orientation (i.e., H<sup>N</sup> and H<sup>2</sup> are *trans* to each other). B) The secondary structure in DMSO solution includes an intramolecular hydrogen bond (dotted line) across the β(1→4) linkage from the amide hydrogen to the adjacent carboxylate group, requiring rotation of the amide sidechain away from the *trans* position [17]. C) In aqueous solution, a water molecule has been proposed to be involved in the secondary structure by forming a hydrogen bonded bridging arrangement between the groups, allowing the amide sidechain to assume the *trans* conformation [18]. D) Schematic depiction of the proposed tertiary structure arrangement of HA in aqueous physiological solution [21, 22]. HA molecules may bind to each other in a repeated antiparallel array, with hydrophobic patches (shaded surfaces) on the faces of the rings (hexagons) stacking against each other and intermolecular hydrogen bonds between amide and carboxylate groups on adjacent molecules (arrows) providing specific stabilisation to the network. The amide group is *trans* in this model and the HA chains are required to adopt an extended two-fold helical conformation.

**Figure 2.** Spectra of HA oligosaccharides at different pH values. A) Titration of the trisaccharide HA<sub>3</sub><sup>NN</sup> (i.e., GlcNAc-GlcA-GlcNAc~OH), showing the pH-dependent migration of amide proton chemical shifts (from α, β and ω residues; refer Figure 3 for nomenclature). B) Overlay of [<sup>1</sup>H-<sup>15</sup>N] HSQC spectra of HA<sub>6</sub>, showing the position of amide resonances at a range of pH values (pH 1.42 to 6.11 ± 0.03). C) Detail of the [<sup>1</sup>H-<sup>15</sup>N] HSQC spectrum of HA<sub>6</sub> at pH ≈ pK<sub>a</sub>, showing the splitting of the γHN resonance caused by an end-effect from the α- and β-anomers. D) Similar detail of the [<sup>1</sup>H-<sup>15</sup>N] HSQC spectrum of HA<sub>4</sub> at pH ≈ pK<sub>a</sub>, showing the splitting of the ωHN resonance.

**Figure 3.** Nomenclature of GlcNAc rings in HA oligosaccharides. Oligomers with an even number of residues and GlcNAc at the reducing terminus (indicated by ~OH) are distinguished by the number of saccharide residues in subscript, i.e., tetrasaccharides, HA<sub>4</sub>; hexasaccharides, HA<sub>6</sub>. Oligomers with an odd number of residues are denoted by the number of residues in subscript and the type of residue at non-reducing and reducing termini in superscript (GlcNAc, GlcA). e.g. GlcNAc-GlcA-GlcNAc~OH = HA<sub>3</sub><sup>NN</sup>; GlcA-GlcNAc-

GlcA-GlcNAc-GlcA~OH = HA<sub>5</sub><sup>AA</sup>. GlcNAc residues are labelled in each oligomer with the Greek alphabet, progressing from the  $\alpha$ - and  $\beta$ -anomers ( $\alpha/\beta$ ) at the reducing terminus through  $\gamma$ ,  $\delta$  etc. on subsequent rings until the centre is reached, while regressing from the non-reducing terminus ( $\omega$ ,  $\psi$ ,  $\phi$  etc.) [5]. Where the central residue is GlcNAc, the assignment is made from the reducing terminal end (e.g. in HA<sub>5</sub><sup>NN</sup>, the sequence of assignments is therefore  $\alpha/\beta$ ,  $\gamma$ ,  $\omega$ , rather than  $\alpha/\beta$ ,  $\psi$ ,  $\omega$ ). Hydroxyl groups have been omitted for clarity.

Figure 4. Chemical shift changes with pH of selected <sup>1</sup>H nuclei in <sup>15</sup>N-HA<sub>6</sub>. The data were fit to one-site models (smooth curves) to determine the apparent pK<sub>a</sub> of the titrating resonance (refer Table 1). The  $\gamma^{\alpha}\text{H}^{\text{N}}$  resonance, which overlaps with  $\gamma^{\beta}\text{H}^{\text{N}}$  at high and low pH (see text), has been omitted for clarity.

Figure 5. 1D spectra of the amide region of HA molecules of various lengths, showing the invariance of the interior amide proton chemical shift with chain length. In HA<sub>8</sub>, end-effects produce fine structure around the basic chemical shift (dotted line), which is largely eclipsed in HA<sub>40</sub>. High molecular-mass HA (HA<sub>2500-8000</sub>, 0.5 - 1.5 MDa) in the presence and absence of physiological NaCl concentrations and at pH values above and below the pK<sub>a</sub> of the carboxylate groups ( $2.9 \pm 0.1$  [31]) has the same chemical shift as the oligomers and a similar line-width to HA<sub>40</sub>.

Figure 6. Strips from a [<sup>1</sup>H-<sup>1</sup>H-<sup>15</sup>N] NOESY-HSQC spectrum of HA<sub>8</sub> (at pH 6.0), showing nuclear Overhauser enhancements (NOEs) from ring protons to each amide proton within the molecule. The peak height intensity of each ring proton NOE is given as a percentage of the corresponding diagonal resonance and all NOEs had the same sign as the diagonal; calculation shows that the error incurred by ignoring spin diffusion is < 10 % on each value. In each strip the H<sup>1</sup> proton of the preceding GlcA ring (i.e., that forming the  $\beta 1 \rightarrow 3$  link) is clearly visible (GlcA H<sup>1</sup>).

Figure 7. Amide-exchange build-up curve for HA<sub>6</sub>, showing the extent of transfer (ordinate) of excited hydrogen nuclei from water to each amide group by chemical exchange after defined periods (abscissa). The raw data have been scaled to  $\beta\text{H}^{\text{N}} = 100\%$  at the last time-point.

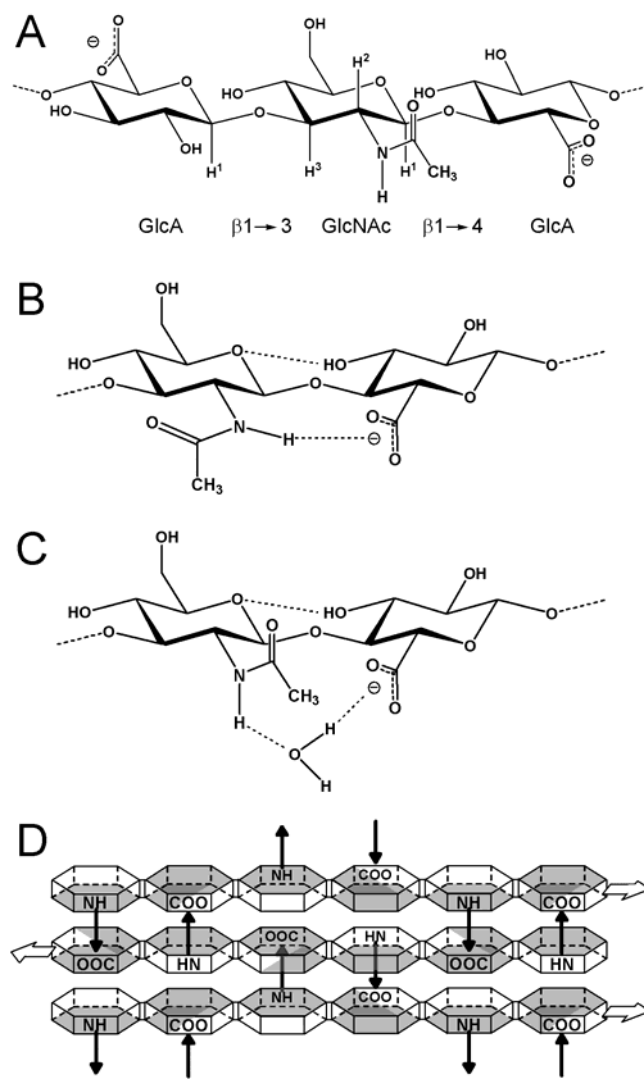


Figure 1

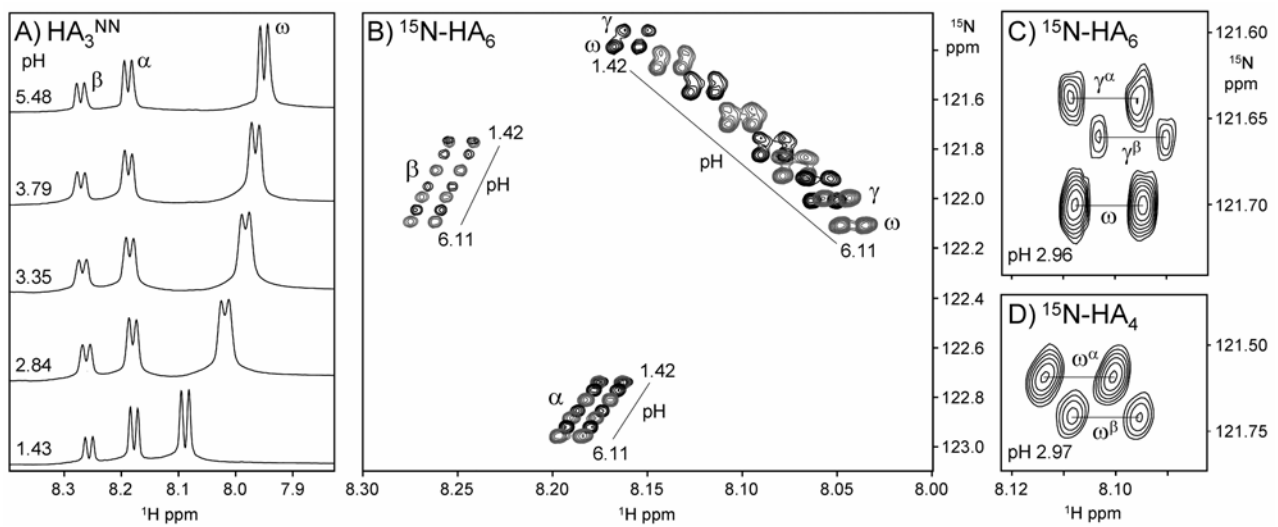


Figure 2

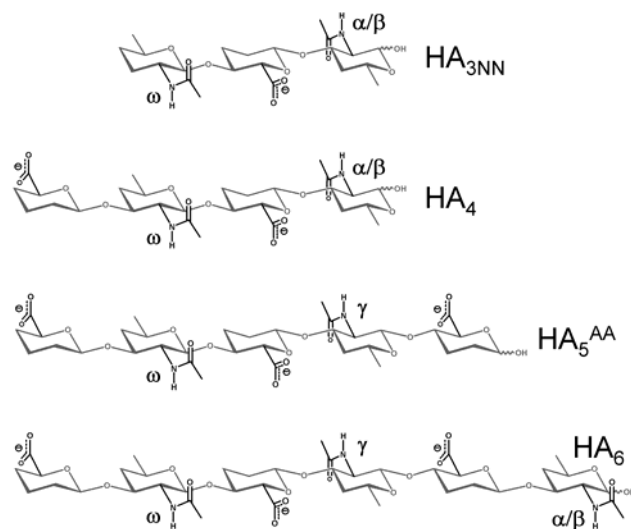


Figure 3

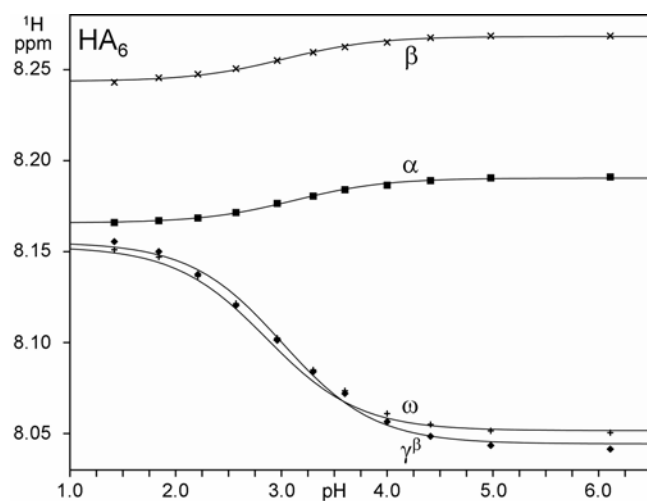


Figure 4

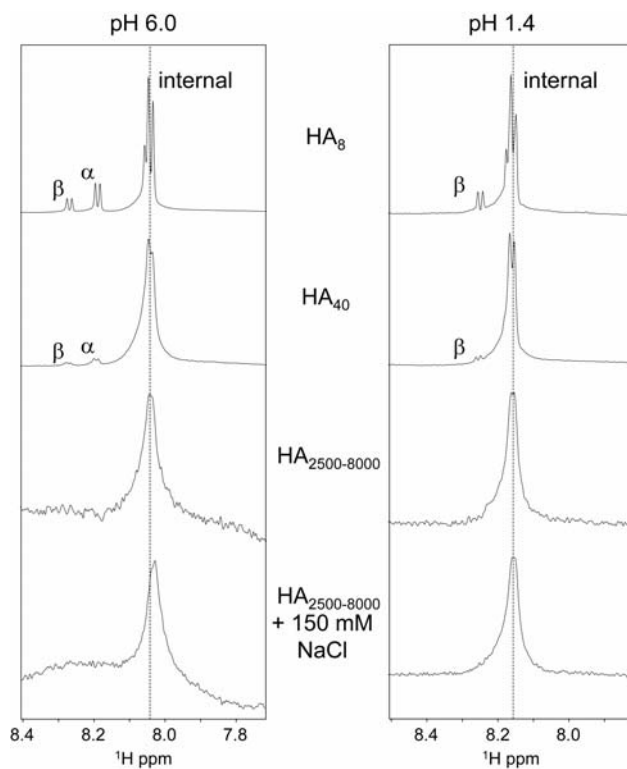


Figure 5

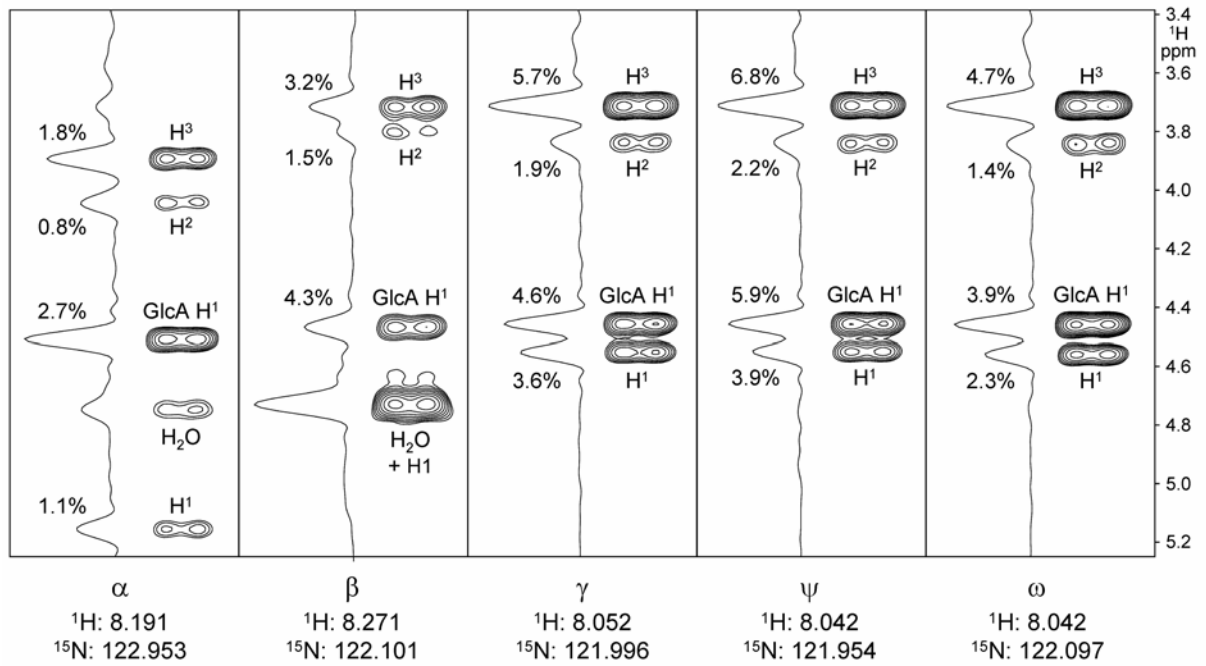


Figure 6

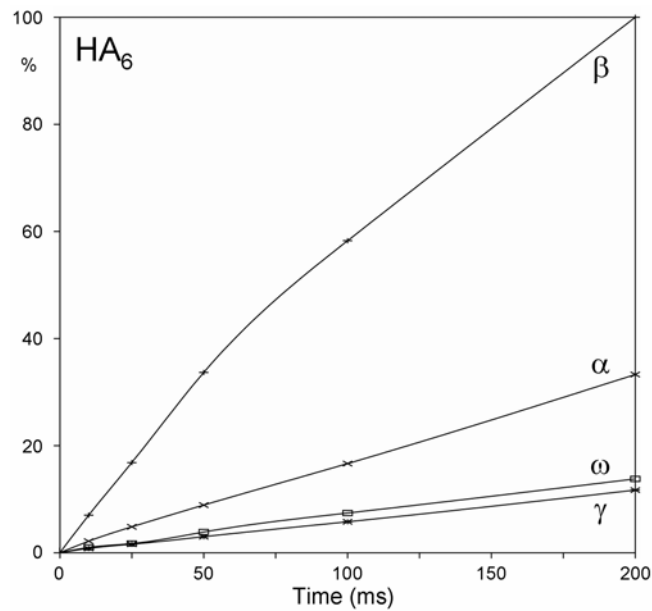


Figure 7